

Autonomous Driving Vehicles Using Adaptive Learning Method for Data Fusion

Farhad Aghili*

Abstract

This paper presents an adaptive learning method for data fusion in autonomous driving vehicles. The localization is based on the integration of Inertial Measurement Unit (IMU) with two Real-Time Kinematic (RTK) Global Positioning System (GPS) units in an adaptive Kalman filter (KF). The observability analysis reveals that *i*) integration of a single GPS with IMU does not constitute an observable system; *ii*) integration of two GPS units with IMU results in a locally observable system provided that the line connecting two GPS antennas is not parallel with the vector of the measured acceleration, i.e., the sum of inertial and gravitational accelerations. The later case makes it possible compensate the error in the estimated orientation due to gyro drift and its bias without needing additional instrument for absolute orientation measurements, e.g., magnetic compass. Moreover, in order to cope with the fact that GPS systems sometimes lose their signal and receive inaccurate position data, the self-tuning filter estimates the covariance matrix associated with the GPS measurement noise. This allows the KF to incorporate GPS measurements in the data fusion process heavily only when the information received by GPS becomes reliably available.

1 Introduction

Both position and attitude determination of a mobile robot are necessary for navigation, guidance and steering control of a mobile robot [1]. *Dead-reckoning* using vehicle kinematic model and incremental measurement of wheel encoders is the common technique to determine the position and orientation of mobile robots for indoors applications [2]. However, the application of these techniques for localization of outdoor robots is limited, particularly when the robot has to traverse an uneven terrain or loose soils. This is because wheel slippage and wheel imperfection cause quick accumulation of the position and attitude errors [3]. Other research utilizes inertial measurement unit and wheel encoders to obtain close estimate of robot position [4–10]. The problem with inertial systems, however, is that they require additional information about absolute position and orientation to overcome long-term drift [11]. Yi *et al.* [10] proposed integration of the kinematic relationship between wheel slip and instantaneous rotation center of skied-steered mobile robots with onboard IMU and wheel encoder to improve motion-estimation accuracy in 2D environment.

*email: faghili@encs.concordia.ca

In essence, to measure the pose of a vehicle with high bandwidth and long-term accuracy and stability usually involves data fusion of different sensors because there is no single sensor to satisfy both requirements. In this respect, GPS and Inertial Measurement Unit are considered complementary positioning systems: GPS systems provide low update rate, but they have the advantage of long-term position accuracy. Conversely, IMU systems provide high bandwidth position information, while they are characterized by long term drift. Additionally, integration of the inertial data continuously provides pose estimation even when the GPS systems lose their signal and receive inaccurate position data namely due to obstruction. Since no wheel odometry is used in this localization method, one can envisage the application of this localization method to humanoid and legged robots as well as aerial vehicles [12].

Nowadays, differential GPSs to centimeter-level accuracy are commercially available making them attractive for localization, guidance and control of outdoor mobile robots [1, 13–17, 17–24]. Improving the accuracy of localization systems using RTK GPS in the presence of GPS latency was addressed in [13]. A localization algorithm based on Kalman filtering to fuse data from a single GPS and other several other sensors and map-based data was presented in [14]. The onboard sensory system includes wheel encodes, inertial navigation system, a laser scanner for relative position measurements and a GPS antenna for absolute pose measurements [25, 26].

An autonomous mobile robot using GPS and photo-sensors was presented in [27]. The feasibility of a low-order vehicle positioning system functioning under an urban environment was investigated in [15]. This positioning system is based on integration of Inertial Navigation System (INS) with a single GPS unit which can provide the vehicle heading angle based on the Doppler effect. Low *et al.* proposed a pose estimator using a single RTK GPS and inertial sensors for motion estimation of a wheeled mobile robot in 2D environment to deal with skidding and slipping problem [18, 19]. However, this sensor fusion method relies on additional instrument for absolute orientation measurements. Similarly, a magnetic compass was incorporated in data fusion of a MEMS-IMU/GPS integrated navigation system proposed in [28] in order to make the heading angle observable. A decentralized data fusion algorithm is presented [22] for simultaneous position estimation of a land vehicle and building the map of the environment by incorporating data from inertial sensor, GPS, laser scanner, the wheel and steering encoders. The majority of the aforementioned techniques for integration of IMU with GPS utilize a single GPS antennas and hence they require additional instrument for absolute orientation measurement, e.g., magnetic compass or laser scanner [29]. Although there are GPS devices that can provide vehicle heading angles based on Doppler effect, the accuracy of the angle measurement drops significantly at low speeds and it does not work at zero speed. Data fusion from multiple sensors has been also utilized for pose estimation of vehicles in aerospace applications [22, 27, 27, 30–34].

This work presents fusing data from an IMU and two RTK GPS units in an adaptive Kalman filter to estimate the attitude, position, and velocity of a vehicle in three-dimensions [1]. Observability analysis of GPS/IMU integration system is investigated in this paper. The results show that the states of the system are observable provided that at least two GPS antennas are utilized and that the line connecting two GPS antennas is not parallel to the acceleration measurement vector [35]. In other words, conventional GPS/IMU integration scheme using one GPS unit is not observable whereas the observability of the integration system using two GPS units can be ensured at the cost of adding an extra GPS unit to the integration system [36]. Moreover, RTK GPS devices notoriously suffer from signal robustness issue as their signal

can be easily disturbed by many factors such as satellite geometry, atmospheric condition and shadow. To deal with the uncertain GPS noise problem, the covariance matrix of the GPS noises is estimated in real-time so that the KF filter incorporates GPS information heavily in the data fusion process only when the GPS measurements become reliably available. Tests have been conducted on the Canadian Space Agency (CSA) *red rover* for assessing the performance of our pose estimator [1]. This paper is organized as follow: Section 2 describes the observation and process models pertaining to the positioning system consisting of two GPSs and an IMU. Observability analysis of such a positioning system is given in Section 2.2. In Section 3, the fusing of accelerometer, rate gyro and GPS information in a self-tuning adaptive KF is developed.

2 Vehicle Sensors and Modelling

Fig. 1 schematically illustrates a vehicle as a rigid body to which two differential GPS-antennas and an IMU device are attached. Coordinate frame $\{\mathcal{A}\}$ is an inertial frame while $\{\mathcal{B}\}$ is a vehicle-fixed (body frame) coordinate system. The origin of frame $\{\mathcal{A}\}$ coincides with that of the GPS base antenna, i.e., the vehicle GPS measurements are expressed in $\{\mathcal{A}\}$. Without loss of generality, we assume that the vehicle body frame, $\{\mathcal{B}\}$, coincides with the IMU coordinate frame, i.e., the IMU measurements are expressed in $\{\mathcal{B}\}$. The orientation of $\{\mathcal{B}\}$ with respect to $\{\mathcal{A}\}$ is represented by the unit quaternion $\mathbf{q} = [\mathbf{q}_v^T \ q_o]^T$, where subscripts v and o denote the vector and scalar parts of the quaternion, respectively. The rotation matrix \mathbf{A} representing the rotation of frame $\{\mathcal{B}\}$ with respect to frame $\{\mathcal{A}\}$ is related to the corresponding quaternion \mathbf{q} by

$$\mathbf{A}(\mathbf{q}) = (2q_o^2 - 1)\mathbf{I}_3 + 2q_o[\mathbf{q}_v \times] + 2\mathbf{q}_v\mathbf{q}_v^T, \quad (1)$$

where $[\cdot \times]$ denotes the matrix form of the cross-product and \mathbf{I}_n denotes the $n \times n$ identity matrix. The quaternion product \otimes is defined as

$$\mathbf{q} \otimes = q_o \mathbf{I}_4 + \mathbf{\Omega}(\mathbf{q}_v) \quad \text{where} \quad \mathbf{\Omega}(\mathbf{q}_v) = \begin{bmatrix} -[\mathbf{q}_v \times] & \mathbf{q}_v \\ -\mathbf{q}_v^T & 0 \end{bmatrix}$$

so that $\mathbf{q}_1 \otimes \mathbf{q}_2$ corresponds to rotation matrix $\mathbf{A}(\mathbf{q}_2)\mathbf{A}(\mathbf{q}_1)$.

2.1 Suite of Sensing Systems

This section first presents the measurement model, followed by the process model including the close-forms of the state transition matrix and the discrete-time process noise needed for covariance propagation. The GPS measurements are directly included in the measurement equations, while the IMU outputs are treated as the time-varying inputs of the process system.

Assume that vector \mathbf{r} represents the location of the origin of frame $\{\mathcal{B}\}$ that is expressed in coordinate frame $\{\mathcal{A}\}$, and \mathbf{p}_i is the output of the i th GPS measurement. Apparently, from Fig. 1, we have

$$\mathbf{p}_i = \mathbf{r} + \mathbf{A}(\mathbf{q})\mathbf{e}_i \quad i = 1, 2 \quad (2)$$

where constant vectors \mathbf{e}_1 and \mathbf{e}_2 are the locations of the corresponding GPS antennas expressed in the IMU frame.

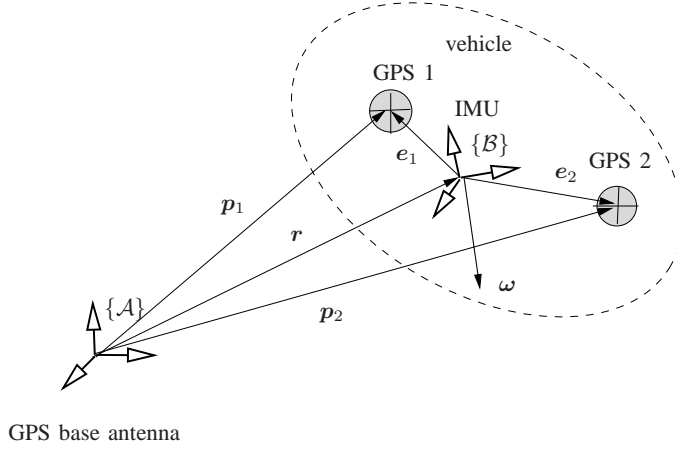


Figure 1: Two GPS antennas and an IMU attached on a vehicle body.

Let us define the state vector to be estimated by the EKF as $\mathbf{x} = [\mathbf{q}_v^T \ \mathbf{r}^T \ \dot{\mathbf{r}}^T \ \mathbf{b}^T]^T$, where vector \mathbf{b} is the gyro bias. Then, one can write the observation vector as a nonlinear function of the state

$$\mathbf{z} = \mathbf{h}(\mathbf{x}) + \mathbf{v},$$

where

$$\mathbf{z} = \begin{bmatrix} \mathbf{p}_1 \\ \mathbf{p}_2 \end{bmatrix}, \quad \mathbf{h}(\mathbf{x}) = \begin{bmatrix} \mathbf{r} + \mathbf{A}(\mathbf{q})\mathbf{e}_1 \\ \mathbf{r} + \mathbf{A}(\mathbf{q})\mathbf{e}_2 \end{bmatrix}, \quad (3)$$

and \mathbf{v} represents the GPS measurement noise, which is assumed random walk with covariance $\mathbf{R} = E[\mathbf{v}\mathbf{v}^T]$.

To linearize the observation vector, $\mathbf{h}(\mathbf{x})$, one needs to derive the sensitivity of the nonlinear observation vector with respect to the system state vector. Consider small variation of the quaternion from its estimation $\hat{\mathbf{q}}$ as

$$\delta\mathbf{q} = \mathbf{q} \otimes \hat{\mathbf{q}}^*, \quad (4)$$

where $\hat{\mathbf{q}}^*$ is the inverse of quaternion $\hat{\mathbf{q}}$, i.e., $\hat{\mathbf{q}}^* \otimes \hat{\mathbf{q}} = [0 \ 0 \ 0 \ 1]^T$. In other words, identity $\mathbf{A}(\mathbf{q}^*) \equiv [\mathbf{A}(\mathbf{q})]^T$ is in order for all quaternion \mathbf{q} . Notice that in the following, the “hat” sign depicts the estimation of a variable. Now, by virtue of $\mathbf{A}(\mathbf{q}) = \mathbf{A}(\delta\mathbf{q} \otimes \hat{\mathbf{q}})$, one can compute the observation vector (3) in terms of the perturbation $\delta\mathbf{q}$. Using the first order approximation of nonlinear matrix function $\mathbf{A}(\delta\mathbf{q})$ from expression (1) by assuming a small rotation $\delta\mathbf{q}$, i.e., $\|\delta\mathbf{q}_v\| \ll 1$ and $\delta q_0 \approx 1$, we will have

$$\mathbf{A}(\delta\mathbf{q}) = \mathbf{I}_3 + 2[\delta\mathbf{q}_v \times] + \text{HOT}. \quad (5)$$

Thus, the sensitivity matrix can be written as

$$\mathbf{H} = \left. \frac{\partial \mathbf{h}}{\partial \mathbf{x}} \right|_{\mathbf{x}=\hat{\mathbf{x}}} = \begin{bmatrix} -2\hat{\mathbf{A}}[\mathbf{e}_1 \times] & \mathbf{I}_3 & \mathbf{0}_3 & \mathbf{0}_3 \\ -2\hat{\mathbf{A}}[\mathbf{e}_2 \times] & \mathbf{I}_3 & \mathbf{0}_3 & \mathbf{0}_3 \end{bmatrix}, \quad (6)$$

where $\hat{\mathbf{A}} = \mathbf{A}(\hat{\mathbf{q}})$.

Denoting the angular velocity of the vehicle by $\boldsymbol{\omega}$, the relation between the time derivative of the quaternion and the angular velocity can be readily expressed by

$$\dot{\mathbf{q}} = \frac{1}{2}\boldsymbol{\Omega}(\boldsymbol{\omega})\mathbf{q} \quad (7)$$

The angular rate is related to the rate gyro measurement by

$$\boldsymbol{\omega} = \mathbf{u}_g + \mathbf{b} + \mathbf{w}_g$$

where \mathbf{u}_g is the gyro output, \mathbf{b} is the gyro bias vector, and \mathbf{w}_g is the angular random walk noise of the gyro rate with covariance $E[\mathbf{w}_g \mathbf{w}_g^T] = \sigma_g^2 \mathbf{I}_3$. The time-derivative of gyro bias is traditionally modeled with random walk model [37,38] according to

$$\dot{\mathbf{b}} = \mathbf{w}_b, \quad (8)$$

where \mathbf{w}_b is the rate random walk noise with covariance $E[\mathbf{w}_b \mathbf{w}_b^T] = \sigma_b^2 \mathbf{I}_3$.

A measurement of the linear acceleration of the vehicle is provided by an accelerometer. We assume that the deterministic error sources of the accelerometer unit, which include scale factor and offset, are compensated. The error can be compensated either internally by its signal processor or externally by a calibration procedure [39]. However, accelerometers cannot distinguish between the acceleration of gravity and inertial acceleration. Therefore, the accelerometer output equation is represented by

$$\ddot{\mathbf{r}} = \mathbf{A}(\mathbf{q})(\mathbf{u}_a + \mathbf{w}_a) - \mathbf{g}, \quad (9)$$

where \mathbf{u}_a is acceleration output, \mathbf{w}_a is the accelerometer noise assumed to be random walk noise \mathbf{w}_a with covariance $E[\mathbf{w}_a \mathbf{w}_a^T] = \sigma_a^2 \mathbf{I}_3$, and \mathbf{g} is the constant gravity vector. Therefore, in view of (7), (8), and (9) the process dynamics can be described by

$$\dot{\mathbf{x}} = \mathbf{f}(\mathbf{x}, \mathbf{u}, \mathbf{w}) \quad (10)$$

where vector $\mathbf{u} = [\mathbf{u}_g^T \ \mathbf{u}_a^T]^T$ contains the IMU outputs, vector $\mathbf{w} = [\mathbf{w}_g^T \ \mathbf{w}_a^T \ \mathbf{w}_b^T]^T$ contains the entire process noise,

$$\mathbf{f}(\mathbf{x}, \mathbf{u}, \mathbf{w}) = \begin{bmatrix} \frac{1}{2} \text{vec}[\boldsymbol{\Omega}(\mathbf{u}_g + \mathbf{b} + \mathbf{w}_g)\mathbf{q}] \\ \dot{\mathbf{r}} \\ \mathbf{A}(\mathbf{q})(\mathbf{u}_a + \mathbf{w}_a) - \mathbf{g} \\ \mathbf{w}_b \end{bmatrix},$$

and $\text{vec}(\cdot)$ returns the vector part of a quaternion.

Although the states can be propagated by solving the nonlinear dynamics equations (10), the state transition matrix of the linearized dynamics equations will be also needed to be used for covariance propagation of the KF [40–42]. Adopting a linearization technique similar to [37,38] one can linearize (7) about the quaternion estimation $\hat{\mathbf{q}}$ and $\hat{\boldsymbol{\omega}} = \hat{\mathbf{u}}_g + \hat{\mathbf{b}}$ to obtain

$$\frac{d}{dt} \delta \mathbf{q}_v = -\hat{\boldsymbol{\omega}} \times \delta \mathbf{q}_v + \frac{1}{2} \delta \mathbf{b} + \frac{1}{2} \mathbf{w}_g \quad (11a)$$

$$\frac{d}{dt} \delta q_o = 0 \quad (11b)$$

Since δq_o is not an independent variable and it has variations of only the second order, its time-derivative can be ignored, as suggested in [37].

Similarly, the equation of translational motion (9) can be linearized about the acceleration estimation, $\hat{\mathbf{a}} = \hat{\mathbf{u}}_a$, and $\hat{\mathbf{q}}$ using the first-order approximation (5) as:

$$\begin{aligned}\delta\dot{\mathbf{r}} &= \mathbf{A}(\delta\mathbf{q} \otimes \hat{\mathbf{q}})(\hat{\mathbf{a}} + \mathbf{w}_a) - \mathbf{A}(\hat{\mathbf{q}})\hat{\mathbf{a}} \\ &\approx -2\hat{\mathbf{A}}[\hat{\mathbf{a}}\times]\delta\mathbf{q}_v + \hat{\mathbf{A}}\mathbf{w}_a.\end{aligned}\quad (12)$$

Thus, setting (8), (11a), and (12) in the state-space form, the linearized model of the continuous system can be derived as

$$\mathbf{F} = \left. \frac{\partial \mathbf{f}}{\partial \mathbf{x}} \right|_{\substack{\mathbf{x} = \hat{\mathbf{x}} \\ \mathbf{u} = \hat{\mathbf{u}}}} = \begin{bmatrix} -[\hat{\boldsymbol{\omega}}\times] & \mathbf{0}_3 & \mathbf{0}_3 & \frac{1}{2}\mathbf{I}_3 \\ \mathbf{0}_3 & \mathbf{0}_3 & \mathbf{I}_3 & \mathbf{0}_3 \\ -2\hat{\mathbf{A}}[\hat{\mathbf{a}}\times] & \mathbf{0}_3 & \mathbf{0}_3 & \mathbf{0}_3 \\ \mathbf{0}_3 & \mathbf{0}_3 & \mathbf{0}_3 & \mathbf{0}_3 \end{bmatrix} \quad (13a)$$

$$\mathbf{G} = \left. \frac{\partial \mathbf{f}}{\partial \mathbf{w}} \right|_{\mathbf{x} = \hat{\mathbf{x}}} = \begin{bmatrix} \frac{1}{2}\mathbf{I}_3 & \mathbf{0}_3 & \mathbf{0}_3 \\ \mathbf{0}_3 & \mathbf{0}_3 & \mathbf{0}_3 \\ \mathbf{0}_3 & \hat{\mathbf{A}} & \mathbf{0}_3 \\ \mathbf{0}_3 & \mathbf{0}_3 & \mathbf{I}_3 \end{bmatrix} \quad (13b)$$

2.2 Observability Analysis

The Kalman filter built around a system whose states are not observable does not simply work [43, 44]. Therefore, a successful use of Kalman filtering requires that the system be observable. A linear time-invariant (LTI) systems is said to be *globally observable* if and only if its observability matrix is full rank. If a system is observable, the estimation error becomes only a function of the system noise, while the effect of the initial values of the states on the error will asymptotically vanish. In that case, the time-varying system (6) and (13a) can be replaced by a piecewise constant system for observability analysis [45, 46]. The intuitive notion is that such a time-varying system can be effectively approximated by a pieces-wise constant system without losing the characteristic behavior of the original system [45, 47].

The section examines the observability of the IMU/GPS integration system for two cases: *i*) two GPS units are incorporated in the sensor fusion; *ii*) a single GPS unit is incorporated.

2.2.1 Adaptive Learning Data Fusion of Multiple Sensors

The observability matrix associated with linearized system (13a) together with the observation model (6) is

$$\mathcal{O} = [\mathbf{H}^T \quad (\mathbf{H}\mathbf{F})^T \quad \dots \quad (\mathbf{H}\mathbf{F}^{11})^T]^T. \quad (14)$$

The states of the system are assumed to be completely observable if and only if

$$\text{rank } \mathcal{O} = 12 \quad (15)$$

which is equivalent to \mathcal{O} having 12 independent rows. Now, let us construct the submatrices of the observability matrix \mathcal{O} from (6) and (13a) as

$$\mathbf{HF} = \begin{bmatrix} 2\hat{\mathbf{A}}[\mathbf{e}_1 \times][\hat{\boldsymbol{\omega}} \times] & \mathbf{0}_3 & \mathbf{I}_3 & -\hat{\mathbf{A}}[\mathbf{e}_1 \times] \\ 2\hat{\mathbf{A}}[\mathbf{e}_2 \times][\hat{\boldsymbol{\omega}} \times] & \mathbf{0}_3 & \mathbf{I}_3 & -\hat{\mathbf{A}}[\mathbf{e}_2 \times] \end{bmatrix} \quad (16a)$$

$$\mathbf{HF}^2 = \begin{bmatrix} -2\hat{\mathbf{A}}([\mathbf{e}_1 \times][\hat{\boldsymbol{\omega}} \times]^2 + [\hat{\mathbf{a}} \times]) & \mathbf{0}_3 & \mathbf{0}_3 & \hat{\mathbf{A}}[\mathbf{e}_1 \times][\hat{\boldsymbol{\omega}} \times] \\ -2\hat{\mathbf{A}}([\mathbf{e}_2 \times][\hat{\boldsymbol{\omega}} \times]^2 + [\hat{\mathbf{a}} \times]) & \mathbf{0}_3 & \mathbf{0}_3 & \hat{\mathbf{A}}[\mathbf{e}_2 \times][\hat{\boldsymbol{\omega}} \times] \end{bmatrix} \quad (16b)$$

$$\mathbf{HF}^3 = \begin{bmatrix} 2\hat{\mathbf{A}}([\mathbf{e}_1 \times][\hat{\boldsymbol{\omega}} \times]^3 + [\hat{\mathbf{a}} \times][\hat{\boldsymbol{\omega}} \times]) & \mathbf{0}_3 & \mathbf{0}_3 & -\hat{\mathbf{A}}([\mathbf{e}_1 \times][\hat{\boldsymbol{\omega}} \times]^2 + [\hat{\mathbf{a}} \times]) \\ 2\hat{\mathbf{A}}([\mathbf{e}_2 \times][\hat{\boldsymbol{\omega}} \times]^3 + [\hat{\mathbf{a}} \times][\hat{\boldsymbol{\omega}} \times]) & \mathbf{0}_3 & \mathbf{0}_3 & -\hat{\mathbf{A}}([\mathbf{e}_2 \times][\hat{\boldsymbol{\omega}} \times]^2 + [\hat{\mathbf{a}} \times]) \end{bmatrix} \quad (16c)$$

By inspection, one can show that \mathbf{HF}^n with $n > 0$ does not produce any additional independent rows and therefore it is sufficient to include only row matrices up to \mathbf{HF}^3 in the observability matrix (14). As shown in the Appendix, the observability matrix can be reduced to the following matrix by few elementary Matrix Row Operations (MRO)

$$\mathcal{O} \xrightarrow{\text{MRO}} \mathcal{O}' = \begin{bmatrix} \mathbf{\Pi} & \mathbf{0}_3 & \mathbf{0}_3 & \mathbf{0}_3 \\ \times & \hat{\mathbf{A}}^T & \mathbf{0}_3 & \mathbf{0}_3 \\ \times & \mathbf{0}_3 & \hat{\mathbf{A}}^T & -[\mathbf{e}_1 \times] \\ \times & \mathbf{0}_3 & \mathbf{0}_3 & \mathbf{\Pi} \end{bmatrix}, \quad (17)$$

where

$$\mathbf{\Pi} = \Delta \mathbf{e} \Delta \mathbf{e}^T [\hat{\mathbf{a}} \times] + [\hat{\mathbf{a}} \times] \quad (18)$$

and vector $\Delta \mathbf{e} = \mathbf{e}_1 - \mathbf{e}_2$ is the antenna-to-antenna baseline vector. If matrix $\mathbf{\Pi}$ is invertible, then the reduced observability matrix \mathcal{O}' can be transformed into a *block-triangular matrix* by pre-multiplying its fourth row by $[\mathbf{e}_1 \times] \mathbf{\Pi}^{-1}$ and then add it to the third row. In which case, the block-triangular matrix is full rank because all of its block diagonal matrices are invertible. Therefore, the full rankness of the reduced observability matrix rests on the invertibility of the square matrix $\mathbf{\Pi}$. In other words, if $\mathbf{\Pi}$ is invertible, then system (6)-(13) is observable.

Proposition 1 *If a line connecting the two GPS antennas is not parallel with the acceleration vector, then system (6)-(13a) is observable.*

PROOF: In a proof by contradiction, we show that $\mathbf{\Pi} \in \mathbb{R}^{3 \times 3}$ must be a full-rank matrix if $\hat{\mathbf{a}} \nparallel \Delta \mathbf{e}$, i.e., vectors $\hat{\mathbf{a}}$ and $\Delta \mathbf{e}$ are not parallel. If $\mathbf{\Pi}$ is not full-rank, then there must exist a non-zero vector $\boldsymbol{\xi} \neq \mathbf{0}$ such that $\mathbf{\Pi} \boldsymbol{\xi} = \mathbf{0}_{3 \times 1}$, which can be written in this form

$$[\boldsymbol{\xi} \times] \Delta \mathbf{e} - \lambda \Delta \mathbf{e} = \mathbf{0}_{3 \times 1} \quad (19)$$

where

$$\lambda = \boldsymbol{\xi}^T (\Delta \mathbf{e} \times \hat{\mathbf{a}}) \quad (20)$$

Notice that (19) is the eigen equation of the skew-symmetric matrix $[\boldsymbol{\xi} \times]$. The only real eigenvalue solution of such skew-symmetric matrix is zero corresponding to eigenvector $\boldsymbol{\xi}$. Therefore, substituting $\lambda = 0$ and $\Delta \mathbf{e} = \boldsymbol{\xi}$ in (20) yields

$$\Delta \mathbf{e} \cdot (\Delta \mathbf{e} \times \hat{\mathbf{a}}) = 0. \quad (21)$$

The only possibility for nonzero vectors $\Delta \mathbf{e}$ and $\hat{\mathbf{a}}$ to satisfy the above identity is that the two vectors are parallel, which is a contradiction. Thus, it is not possible for $\mathbf{\Pi}\boldsymbol{\xi} = \mathbf{0}$ to be true, meaning that matrix $\mathbf{\Pi}$ is full rank and hence so is the observability matrix.

It is worth mentioning that the angle made by two vectors $\Delta \mathbf{e}$ and $\hat{\mathbf{a}}$ can be calculated by

$$\theta = \cos^{-1} \frac{|\Delta \mathbf{e} \cdot \hat{\mathbf{a}}|}{\|\Delta \mathbf{e}\| \|\hat{\mathbf{a}}\|}. \quad (22)$$

The above identity can be used in real-time to check if the observability matrix is close to the ill-condition $\theta = 0$. Clearly, if the vehicle remains stationary, i.e., $\dot{\mathbf{r}} = \ddot{\mathbf{r}} = \mathbf{0}_{3 \times 1}$, the acceleration output $\hat{\mathbf{a}}$ contains only the gravitational acceleration component. In this case, the pose estimator is simply observable if the antenna-to-antenna baseline is not parallel to the gravity vector.

2.2.2 Single-GPS/IMU Integration

Now, assume that only one GPS measurement is available, say GPS 1. Then, the sensitivity matrix matrix becomes

$$\mathbf{H} = [-2\hat{\mathbf{A}}[\mathbf{e}_1 \times] \quad \mathbf{I}_3 \quad \mathbf{0}_3 \quad \mathbf{0}_3]. \quad (23)$$

Consequently, the first rows of the corresponding matrices in (16) constitute $\mathbf{H}\mathbf{F}$ to $\mathbf{H}\mathbf{F}^3$ matrices of the new observability matrix. By inspection, one can see that non-zero vector

$$\boldsymbol{\eta} = \begin{bmatrix} \hat{\mathbf{a}} \\ 2\hat{\mathbf{A}}(\mathbf{e}_1 \times \hat{\mathbf{a}}) \\ \mathbf{0}_{3 \times 1} \\ 2\hat{\boldsymbol{\omega}} \times \hat{\mathbf{a}} \end{bmatrix}$$

lies in the null-space of the new observability matrix \mathcal{O} because

$$\mathcal{O}\boldsymbol{\eta} = \mathbf{0}_{12 \times 1}. \quad (24)$$

This means that matrix \mathcal{O} is not full rank and hence system (23)-(13a) is not observable. In other words, at least two GPS antennas are required for the IMU/GPS integration system to be observable.

3 Adaptive Data Fusion

The equivalent discrete-time model of the linearized system (13) is also required for the Kalman filter design. The state transition matrix over time interval t_Δ is given by

$$\boldsymbol{\Phi}(t_k + t_\Delta, t_k) = \boldsymbol{\Phi}_k = e^{\mathbf{F}(t_k)t_\Delta} \quad (25)$$

Then, using the sinusoidal solution of the matrix exponential of the cross-product [37, 38], the state transition matrix $\boldsymbol{\Phi}_k(\tau) = \boldsymbol{\Phi}(t_k + \tau, t_k)$ can be obtained by solving the matrix exponential problem (25) as

$$\boldsymbol{\Phi}_k(\tau) = \begin{bmatrix} \boldsymbol{\Lambda}_k(\tau) & \mathbf{0}_3 & \mathbf{0}_3 & \frac{1}{2}\boldsymbol{\Lambda}'_k(\tau) \\ \mathbf{0}_3 & \mathbf{0}_3 & \mathbf{I}_3\tau & \mathbf{0}_3 \\ -\hat{\mathbf{A}}_k[\hat{\mathbf{a}}_k \times] \boldsymbol{\Lambda}'_k(\tau) & \mathbf{0}_3 & \mathbf{0}_3 & \mathbf{0}_3 \\ \mathbf{0}_3 & \mathbf{0}_3 & \mathbf{0}_3 & \mathbf{I}_3 \end{bmatrix}.$$

where the submatrices of the above matrix are given by

$$\begin{aligned}\Lambda_k(\tau) &= \mathbf{I}_3 - \frac{\sin \|\hat{\boldsymbol{\omega}}_k\| \tau}{\|\hat{\boldsymbol{\omega}}_k\|} [\hat{\boldsymbol{\omega}}_k \times] + \frac{1 - \cos \|\hat{\boldsymbol{\omega}}_k\| \tau}{\|\hat{\boldsymbol{\omega}}_k\|^2} [\hat{\boldsymbol{\omega}}_k \times]^2 \\ \Lambda'_k(\tau) &= \mathbf{I}_3 \tau + \frac{\cos \|\hat{\boldsymbol{\omega}}_k\| \tau - 1}{\|\hat{\boldsymbol{\omega}}_k\|^2} [\hat{\boldsymbol{\omega}}_k \times] + \frac{\|\hat{\boldsymbol{\omega}}_k\| \tau - \sin \|\hat{\boldsymbol{\omega}}_k\| \tau}{\|\hat{\boldsymbol{\omega}}_k\|^3} [\hat{\boldsymbol{\omega}}_k \times]^2\end{aligned}$$

The IMU noise constitutes the continuous process noise of the entire system with covariance

$$E[\mathbf{w} \mathbf{w}^T] = \boldsymbol{\Sigma}_{\text{imu}} = \text{diag}(\sigma_g^2 \mathbf{I}_3, \sigma_a^2 \mathbf{I}_3, \sigma_b^2 \mathbf{I}_3).$$

The covariance matrix of the discrete-time process noise, which will be used by the KF, can be calculated by [48]

$$\mathbf{Q}_k = \int_0^{t_\Delta} \Phi_k(\tau) \mathbf{G} \boldsymbol{\Sigma}_{\text{imu}} \mathbf{G}^T \Phi_k^T(\tau) d\tau. \quad (26)$$

Using the first-order approximation of the matrix exponential as $\Phi_k(\tau) = e^{\mathbf{F}(t_k)\tau} \approx \mathbf{I}_{12} + \mathbf{F}(t_k)\tau$ in (26) yields the covariance matrix in the following form

$$\mathbf{Q}_k = \begin{bmatrix} \mathbf{Q}_{k11} & \times & \times & \times \\ \mathbf{0}_3 & \mathbf{0}_3 & \times & \times \\ \mathbf{Q}_{k31} & \mathbf{0}_3 & \mathbf{Q}_{k33} & \times \\ \frac{1}{4}\sigma_b^2 t_\Delta^2 \mathbf{I}_3 & \mathbf{0}_3 & \mathbf{0}_3 & \sigma_b^2 t_\Delta \mathbf{I}_3 \end{bmatrix},$$

where

$$\begin{aligned}\mathbf{Q}_{k11} &= \left(\frac{\sigma_b^2 t_\Delta^3}{12} + \frac{\sigma_g^2 t_\Delta}{6}\right) \mathbf{I}_3 - \frac{\sigma_g^2 t_\Delta^3}{12} [\hat{\boldsymbol{\omega}}_k \times]^2 \\ \mathbf{Q}_{k31} &= \frac{\sigma_g^2 t_\Delta}{4} \mathbf{I}_3 + \frac{\sigma_g^2 t_\Delta^2}{8} ([\hat{\boldsymbol{\omega}}_k \times] - 2\hat{\mathbf{A}}_k[\hat{\mathbf{a}}_k \times]) - \frac{\sigma_g^2 t_\Delta^3}{6} \hat{\mathbf{A}}_k[\hat{\mathbf{a}}_k \times][\hat{\boldsymbol{\omega}}_k \times] \\ \mathbf{Q}_{k33} &= \left(\sigma_a^2 + \frac{\sigma_g^2}{4}\right) t_\Delta \mathbf{I}_3 - \frac{\sigma_g^2 t_\Delta^3}{3} \hat{\mathbf{A}}_k[\hat{\mathbf{a}}_k \times] \hat{\mathbf{A}}_k^T + \frac{\sigma_g^2 t_\Delta^2}{4} ([\hat{\mathbf{a}}_k \times] \hat{\mathbf{A}}_k^T - \hat{\mathbf{A}}_k[\hat{\mathbf{a}}_k \times]).\end{aligned}$$

Now, one can design an extended Kalman filter based on the derived models. Let us assume that the state vector is partitioned as $\mathbf{x} = [\mathbf{q}_v^T \boldsymbol{\chi}^T]^T$, where $\boldsymbol{\chi} = [\mathbf{r}^T \dot{\mathbf{r}}^T \mathbf{b}^T]^T$ is the part of the state vector which excludes the quaternion. Then, the EKF-based observer for the associated linearized system (6)-(13) is given in two steps: (i) estimate propagation

$$\hat{\mathbf{x}}_{k/k-1} = \hat{\mathbf{x}}_{k-1} + \int_{t_k}^{t_k+t_\Delta} \mathbf{f}(\mathbf{x}, \mathbf{u}(\tau), \mathbf{0}) d\tau \quad (27a)$$

$$\mathbf{P}_{k/k-1} = \Phi_{k-1} \mathbf{P}_{k-1} \Phi_{k-1}^T + \mathbf{Q}_{k-1} \quad (27b)$$

and (ii) estimate correction

$$\mathbf{K}_k = \mathbf{P}_{k/k-1} \mathbf{H}_k^T (\mathbf{H}_k \mathbf{P}_{k/k-1} \mathbf{H}_k^T + \mathbf{R}_k)^{-1} \quad (28a)$$

$$\Delta \hat{\mathbf{x}}_k = \mathbf{K} (\mathbf{z}_k - \mathbf{h}(\hat{\mathbf{x}}_{k/k-1})) \quad (28b)$$

$$\mathbf{P}_k = (\mathbf{I}_{15} - \mathbf{K}_k \mathbf{H}_k) \mathbf{P}_{k/k-1} \quad (28c)$$

where $\hat{\mathbf{x}}_{k/k-1}$ and $\hat{\mathbf{x}}_k$ are *a priori* and *a posteriori* estimations of the state vector, and $\mathbf{H}_k = \mathbf{H}(\hat{\mathbf{x}}_{k/k-1})$. The state update follows the error-state update, $\Delta\hat{\mathbf{x}} = [\Delta\hat{\mathbf{q}}_v^T \Delta\hat{\boldsymbol{\chi}}^T]^T$, in the *innovation step* of the Kalman filter (28b). The update of "non-quaternion part" of the state vector, i.e. $\hat{\boldsymbol{\chi}}$, can be easily obtained by adding the corresponding error to a priori estimation. However, quaternion update is more complicated because only the vectors parts of the quaternion error $\Delta\hat{\mathbf{q}}_v$ is given at every step time. Therefore, firstly, the scalar part of the quaternion variation should be computed from the corresponding vector part. Secondly, the quaternion update is computed using the quaternion multiplication rule. Consequently, the state update may proceed right after (28b) as

$$\begin{aligned}\hat{\boldsymbol{\chi}}_k &= \Delta\hat{\boldsymbol{\chi}}_k + \hat{\boldsymbol{\chi}}_{k/k-1} \\ \hat{\mathbf{q}}_k &= \left[\frac{\Delta\hat{\mathbf{q}}_{v_k}}{\sqrt{1 - \|\Delta\hat{\mathbf{q}}_{v_k}\|^2}} \right] \otimes \hat{\mathbf{q}}_{k/k-1}\end{aligned}\quad (29)$$

Covariance propagation in (27b) relies on the values of state transition matrix of the discrete-time system, which is linearized about the estimations of the states and the inputs at time t_{k-1} , i.e., $\boldsymbol{\Phi}_{k-1} = \boldsymbol{\Phi}(\hat{\mathbf{x}}_{k-1}, \hat{\mathbf{u}}_{k-1})$. The sampling rate of IMU signals are usually higher than those of GPS signals. Therefore, the input estimation at every step time can be obtained from averaging of IMU signals between two consecutive GPS data acquisition in the interval $t_k < t \leq t_k + t_\Delta$. That is,

$$\hat{\mathbf{u}}_{k-1} = \frac{1}{t_\Delta} \int_{t_{k-1}}^{t_{k-1}+t_\Delta} \mathbf{u}(\tau) d\tau.$$

Notice that incorporation of the decimated IMU signals in derivation of the state transition matrix is a good approximation to be used only for covariance propagation. However, the position and orientation states are propagated separately by integration of the IMU inputs at the original sampling rate in the state propagation step (27a).

3.1 Estimation of Noise Covariance

Efficient implementation of the KF requires the statistical characteristics of the measurement and process noises. The covariances of the IMU noises can be treated as a constant parameter, which can be either derived from the sensor specification or empirically tuned. However, the GPS measurement errors may vary from one point to the next, in which case the error depends on many factors such as satellite geometry, atmospheric condition, multipath areas, and shadow. Therefore, since the covariance matrix associated with the GPS noise is not known beforehand, it has to be estimated in the filter's internal model, so that the filter is "tuned" as much as possible [49].

In a noise-adaptive Kalman filter, the issue is that, in addition to the states, the covariance matrix of the measurement noise has to be estimated [49, 50]. The fundamental assumption on which the adaptive Kalman filter is based is that the innovation sequence can be effectively approximated as an ergodic process inside a sliding sampling window with length w . Let us define the residual error, $\boldsymbol{\rho}_k$, which is obtained from the incoming GPS data information \mathbf{z}_k and the optimal *a posteriori* state estimates $\hat{\mathbf{x}}_{k/k-1}$ according to

$$\boldsymbol{\rho}_k = \mathbf{z}_k - \mathbf{H}_k \hat{\mathbf{x}}_{k/k-1}. \quad (30)$$

The above equation can be equivalently written as

$$\boldsymbol{\rho}_k = \mathbf{H}_k(\mathbf{x}_k - \hat{\mathbf{x}}_{k/k-1}) + \mathbf{v}_k. \quad (31)$$

Taking variance of both sides of (31) gives

$$\mathbf{R}_k = \mathbf{S}_k - \mathbf{H}_k \mathbf{P}_{k/k-1} \mathbf{H}_k^T \quad \text{with} \quad \mathbf{S}_k = E[\boldsymbol{\rho}_k \boldsymbol{\rho}_k^T]. \quad (32)$$

The above equation can be used to estimate the measurement covariance matrix $\hat{\mathbf{R}}_k$ from an ergodic approximation of the covariance of the zero-mean residual $\boldsymbol{\rho}$ in the sliding sampling window with finite length w . That is

$$\hat{\mathbf{S}}_k \approx \frac{1}{w} \sum_{i=k-w}^k \boldsymbol{\rho}_i \boldsymbol{\rho}_i^T \quad (33)$$

where w is chosen empirically to give some statistical smoothing [51]. The intuitive motion in choosing a finite window in the estimation of the innovation covariance matrix is that very past error data has to be discounted when being used for estimation of the current covariance. It is known that if the innovation sequence can be assumed to be essentially time-invariant (ergodic) over the most recent w steps, then using (33) in (32) yields optimal estimation of the covariance matrix $\hat{\mathbf{R}}_k$ in the sliding sampling window [51]. Then, the expression for recursive estimation of the covariance matrix is given by

$$\hat{\mathbf{S}}_k = \begin{cases} \frac{k-1}{k} \hat{\mathbf{S}}_{k-1} + \frac{1}{k} \boldsymbol{\rho}_k \boldsymbol{\rho}_k^T & \text{if } k < w \\ \hat{\mathbf{S}}_{k-1} + \frac{1}{w} (\boldsymbol{\rho}_k \boldsymbol{\rho}_k^T - \boldsymbol{\rho}_{k-w} \boldsymbol{\rho}_{k-w}^T) & \text{otherwise} \end{cases} \quad (34)$$

To summarize, the adaptive estimator for driftless pose estimation of a vehicle by fusing two RTK GPSs and IMU is schematically illustrated in Fig. 2.

3.2 Initialization

For the first iteration of the EKF, an adequate guess of the initial states is required. The initial position and orientation of the vehicle at $t = 0$ s have to be carefully selected to keep the initial error in pose estimate as small as possible based on the information available from the measurements.

Let us form the following matrices:

$$\begin{aligned} \mathbf{M} &= [\Delta \mathbf{p}(0) \quad \mathbf{g} \quad \Delta \mathbf{p}(0) \times \mathbf{g}] \\ \mathbf{N} &= [\Delta \mathbf{e} \quad \hat{\mathbf{u}}_a(0) \quad \Delta \mathbf{e} \times \hat{\mathbf{u}}_a(0)] \end{aligned} \quad (35)$$

where $\Delta \mathbf{p}(0) \triangleq \mathbf{p}_1(0) - \mathbf{p}_2(0)$ is difference between the two GPS outputs at initial time $t = 0$. In view of (2), one can say that vector $\Delta \mathbf{p}$ is the rotated version of vector $\Delta \mathbf{e}$ if GPS noises are ignored. Moreover, in static case, where $\dot{\mathbf{r}}(0) \equiv \ddot{\mathbf{r}}(0) \equiv \mathbf{0}$, we can say vector $\mathbf{u}_a(0)$ is the rotated version of \mathbf{g} if the accelerometer noise is ignored too. Under these circumstances, the above two matrices are simply related by the rotation matrix as

$$\mathbf{M} = \mathbf{A} \mathbf{N} \quad (36)$$

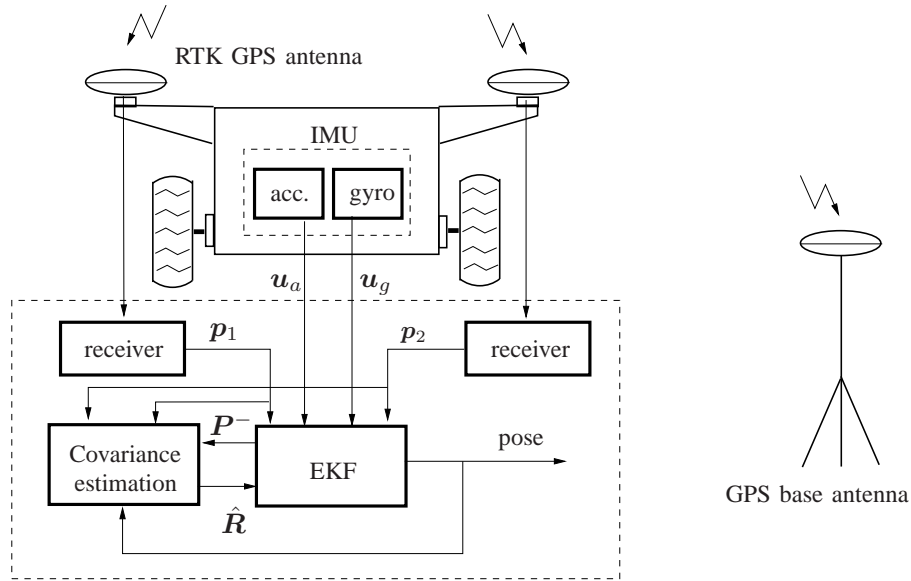


Figure 2: The block diagram of the attitude determination and localization of a vehicle.

Matrices \mathbf{M} and \mathbf{N} are non singular as long as \mathbf{g} and $\Delta\mathbf{p}(0)$ are not collinear, i.e., the line connecting the GPS antennas is not parallel to the gravity vector. Then, the rotation matrix can be obtained from matrix inversion as

$$\mathbf{A} = \mathbf{M}\mathbf{N}^{-1} \quad (37)$$

Solution (37) yields a valid rotation matrix \mathbf{A} so that $\mathbf{A}^T\mathbf{A} = \mathbf{I}_3$ only if there is no error in the column vectors of matrices (35). This may not be the case in practice, however, due to the IMU and GPS noises. To correct this problem, one may observe that all singular values of any orthogonal matrix must be one. This means that the singular value decomposition of the right-hand-side of (37) yields

$$\mathbf{M}\mathbf{N}^{-1} = \mathbf{U}\mathbf{\Sigma}\mathbf{V}^T,$$

where \mathbf{U} and \mathbf{V} are orthogonal matrices and matrix $\mathbf{\Sigma} = \mathbf{I}_3 + \mathbf{\Delta}_{\Sigma}$ is expected to be close to the identity matrix, i.e., $\|\mathbf{\Delta}_{\Sigma}\| \ll 1$. Therefore, by ignoring small matrix $\mathbf{\Delta}_{\Sigma}$, a valid solution for the initial rotation matrix can be found as

$$\mathbf{A}(0) = \mathbf{U}\mathbf{V}^T, \quad (38)$$

which, then, can be used to obtain the equivalent quaternion at $t = 0$ s.

Now, with the initial guess of the rotation matrix in hand, one can obtain the initial guess of the position from (1) as

$$\mathbf{r}(0) = \frac{1}{2}(\mathbf{p}_1(0) + \mathbf{p}_2(0)) - \frac{1}{2}\mathbf{A}(0)(\mathbf{e}_1 + \mathbf{e}_2).$$

4 Conclusions

A adaptive learning method of data fusion in autonomous diving vehicles has been presented. 3D attitude determination and positioning of vehicles by fusing the information from a two RTK

GPS units and an IMU in an adaptive KF has been developed. Examining the observability of different GPS/IMU integration systems has revealed that *i*) the single-GPS/IMU integration system is not observable, *ii*) the dual-GPS/IMU integration system is locally observable provided that the line connecting two GPS antennas is not parallel with the vector of the measured acceleration. Therefore, the dual-GPS/IMU integration method enabled the Kalman filter to compensate for the gyro drift in the data fusion process without using additional instrument for absolute orientation measurements, such as magnetic compass. Moreover, since the attitude estimation method did not rely on the heading angle measurement from the Doppler shift, it worked at low or zero speeds. In addition to the vehicle's position and orientation, the KF estimator was able to estimate the covariance of the GPS measurement noises in real time. This allowed to incorporate the GPS measurement heavily in the data fusion process only when GPS data became reliably available. A method for adequate initialization of the KF has been developed for fast and reliable convergence of the estimator.

The following matrix,

$$\mathcal{O} \xrightarrow{\text{MRO}} \begin{bmatrix} [\Delta \mathbf{e} \times] & \mathbf{0}_3 & \mathbf{0}_3 & \mathbf{0}_3 \\ \mathbf{e}_1^T [\hat{\mathbf{a}} \times] & \mathbf{0}_{1 \times 3} & \mathbf{0}_{1 \times 3} & \mathbf{0}_{1 \times 3} \\ -\mathbf{e}_2^T [\hat{\mathbf{a}} \times] & \mathbf{0}_{1 \times 3} & \mathbf{0}_{1 \times 3} & \mathbf{0}_{1 \times 3} \\ \times & \hat{\mathbf{A}}^T & \mathbf{0}_3 & \mathbf{0}_3 \\ \times & \mathbf{0} & \hat{\mathbf{A}}^T & -[\mathbf{e}_1 \times] \\ \times & \mathbf{0}_3 & \mathbf{0}_3 & [\Delta \mathbf{e} \times] \\ \times & \mathbf{0}_{1 \times 3} & \mathbf{0}_{1 \times 3} & \mathbf{e}_1^T [\hat{\mathbf{a}} \times] \\ \times & \mathbf{0}_{1 \times 3} & \mathbf{0}_{1 \times 3} & -\mathbf{e}_2^T [\hat{\mathbf{a}} \times] \end{bmatrix},$$

can be constructed via the following elementary operations: The first row of the above matrix is obtained by pre-multiplying the first and second rows of \mathbf{H} in (6) by $\hat{\mathbf{A}}^T$ and then subtracting the resultant row vectors. The second and third rows of the above matrix are obtained by pre-multiplying the first and second rows of $\mathbf{H}\mathbf{F}^2$ in (16b) by $-\frac{1}{2}[\hat{\mathbf{A}}\mathbf{e}_1]^T$ and by $\frac{1}{2}[\hat{\mathbf{A}}\mathbf{e}_2]^T$, respectively. The fourth and fifth rows are obtained pre-multiplying the first rows of \mathbf{H} in (6) and $\mathbf{H}\mathbf{F}$ in (16a) by $\hat{\mathbf{A}}^T$. The sixth row is obtained by pre-multiplying the first and second rows of $\mathbf{H}\mathbf{F}$ in (16a) by $\hat{\mathbf{A}}^T$ and then subtracting the resultant row vectors. Finally, the seventh and eighth rows are obtained by pre-multiplying the first and second rows of $\mathbf{H}\mathbf{F}^3$ in (16c) by $[\hat{\mathbf{A}}\mathbf{e}_1]^T$ and $-[\hat{\mathbf{A}}\mathbf{e}_2]^T$, respectively. Notice that the following identity

$$\mathbf{e}_i^T [\mathbf{e}_i \times] = \mathbf{0} \quad \forall i = 1, 2.$$

was used in the above derivations. Adding the second and third rows of the above matrix and pre-multiplying the resultant row by $\Delta \mathbf{e}$ and repeating the operation for the seventh and eighth rows yields

$$\xrightarrow{\text{MRO}} \begin{bmatrix} [\Delta \mathbf{e} \times] & \mathbf{0}_3 & \mathbf{0}_3 & \mathbf{0}_3 \\ \Delta \mathbf{e} \Delta \mathbf{e}^T [\hat{\mathbf{a}} \times] & \mathbf{0}_3 & \mathbf{0}_3 & \mathbf{0}_3 \\ \times & \hat{\mathbf{A}}^T & \mathbf{0}_3 & \mathbf{0}_3 \\ \times & \mathbf{0}_3 & \hat{\mathbf{A}}^T & -[\mathbf{e}_1 \times] \\ \times & \mathbf{0}_3 & \mathbf{0}_3 & [\Delta \mathbf{e} \times] \\ \times & \mathbf{0}_3 & \mathbf{0}_3 & \Delta \mathbf{e} \Delta \mathbf{e}^T [\hat{\mathbf{a}} \times] \end{bmatrix}, \quad (39)$$

Now, one can readily show that by adding the first and second rows of matrix (39) and then adding the fifth and sixth rows of matrix (39), the matrix is reduced to (17).

References

- [1] F. Aghili and A. Salerno, “Driftless 3D attitude determination and positioning of mobile robots by integration of IMU with two RTK GPSs,” *IEEE/ASME Trans. on Mechatronics*, vol. 18, no. 1, pp. 21–31, Feb. 2013.
- [2] P. Oryschuk, A. Salerno, A. M. Al-Husseini, and J. Angeles, “Experimental validation of an underactuated two-wheeled mobile robot,” *IEEE/ASME Trans. on Mechatronics*, vol. 14, no. 2, pp. 252–257, 2009.
- [3] L. Kleeman, “Optimal estimation of position and heading for mobile robots using ultrasonic beacons and dead-reckoning,” in *IEEE Int. Conference on Robotics & Automation*, Nice, France, May 1992, pp. 2582–2587.
- [4] J. Vaganay, M. J. Aldon, and A. Fournier, “Mobile robot attitude estimation by fusion of inertial data,” in *IEEE Int. Conference on Robotics & Automation*, Atlanta, GA, May 1993, pp. 277–282.
- [5] Y. Fuke and E. Krotkov, “Dead reckoning for a lunar rover on uneven terrain,” in *IEEE Int. Conference on Robotics & Automation*, Minneapolis, Minnesota, April 1996, pp. 411–416.
- [6] H. Chung, L. Ojeda, and J. Borenstein, “Accurate mobile robot dead-reckoning with a precision-calibrated fiber-optic gyroscope,” *IEEE Tran. on Robotics & Automation*, vol. 17, no. 1, pp. 80–84, February 2001.
- [7] G. Dissanayake, S. Sukkarieh, E. Nebot, and H. Durrant-Whyte, “The aiding of a low-cost strapdown inertial measurement unit using vehicle model constraints for land vehicle applications,” *IEEE Trans. on Robotics & Automation*, vol. 17, no. 5, pp. 731–747, 2001.
- [8] J. Yi, J. Zhang, D. Song, and S. Jayasuriya, “IMU-based localization and slip estimation for skid-steered mobile robots,” in *IEEE/RSJ Int. Conference on Intelligent Robots and Systems*, San Diego, CA, Oct. 29–Nov. 2 2007, pp. 2845–2850.
- [9] S. Lazarus, I. Ashokaraj, A. Tsourdos, R. Zbikowski, P. Silson, N. Aouf, and B. A. White, “Vehicle localization using sensors data fusion via integration of covariance intersection and interval analysis,” *Sensors Journal, IEEE*, vol. 7, no. 9, pp. 1302–1314, sep. 2007.
- [10] J. Yi, H. Wang, J. Zhang, D. Song, S. Jayasuriya, and J. Liu, “Kinematic modeling and analysis of skid-steered mobile robots with applications to low-cost inertial-measurement-unit-based motion estimation,” *Robotics, IEEE Transactions on*, vol. 25, no. 5, pp. 1087–1097, 2009.
- [11] B. Barshan and H. F. Durrant-Whyte, “Inertial navigation systems for mobile robots,” *IEEE Trans. on Robotics & Automation*, vol. 11, no. 3, pp. 328–342, June 1995.
- [12] A. Shaw and D. Barnes, “Landmark recognition for localisation and navigation of aerial vehicles,” in *IEEE/RSJ International Conf. on Intelligent Robots & Systems*, Las Vegas, Nevada, Oct. 2003, pp. 42–47.

- [13] D. Bouvet and G. Garcia, “Improving the accuracy of dynamic localization systems using RTK GPS by identifying the GPS latency,” in *IEEE Int. Conf. On Robotics and Automation*, San Francisco, CA, April 2000.
- [14] S. Panzieri, F. Pascucci, and G. Ulivi, “An outdoor navigation system using gps and inertial platform,” *Mechatronics, IEEE/ASME Transactions on*, vol. 7, no. 2, pp. 134–142, jun. 2002.
- [15] J. Huang and H.-S. Tan, “A low-order DGPS-based vehicle positioning system under urban environment,” *Mechatronics, IEEE/ASME Transactions on*, vol. 11, no. 5, pp. 567–575, oct. 2006.
- [16] J. I. Meguro, J. I. Takiguchi, Y. Amano, and T. Hashizume, “3D reconstruction using multibaseline omnidirectional motion stereo based on GPS/dead-reckoning compound navigation system,” *International Journal of Robotics Research*, vol. 26, no. 6, pp. 625–636, 2007.
- [17] F. Aghili and A. Salerno, “Attitude determination and localization of mobile robots using two RTK GPSs and IMU,” in *IEEE/RSJ International Conference on Intelligent Robots & Systems*, St. Louis, USA, October 2009, pp. 2045–2052.
- [18] C. B. Low and D. Wang, “Integrated estimation for wheeled mobile robot posture, velocities, and wheel skidding perturbations,” in *Robotics and Automation, 2007 IEEE International Conference on*, 2007, pp. 2355–2360.
- [19] —, “Gps-based tracking control for a car-like wheeled mobile robot with skidding and slipping,” *Mechatronics, IEEE/ASME Transactions on*, vol. 13, no. 4, pp. 480–484, aug. 2008.
- [20] S. Shair, J. H. Chandler, V. J. Gonzalez-Villela, R. M. Parkin, and M. R. Jackson, “The use of aerial images and gps for mobile robot waypoint navigation,” *Mechatronics, IEEE/ASME Transactions on*, vol. 13, no. 6, pp. 692–699, dec. 2008.
- [21] H. J. Woo, B. J. Yoon, B. G. Cho, and J. H. Kim, “Research into navigation algorithm for unmanned ground vehicle using real time kinematic (RTK)-GPS,” in *IEEE ICCAS-SICE*, Fukuoka, Japan, August 2009.
- [22] E. Asadi and M. Bozorg, “A decentralized architecture for simultaneous localization and mapping,” *Mechatronics, IEEE/ASME Transactions on*, vol. 14, no. 1, pp. 64–71, feb. 2009.
- [23] L. Yang, Z. Guo, Y. Li, and C. Li, “Posture measurement and coordinated control of twin hoisting-girder transporters based on hybrid network and rtk-gps,” *Mechatronics, IEEE/ASME Transactions on*, vol. 14, no. 2, pp. 141–150, apr. 2009.
- [24] F. Aghili and A. Salerno, “3-D localization of mobile robots and its observability analysis using a pair of RTK GPSs and an IMU,” in *IEEE/ASME Int. Conf. on Advanced Intelligent Mechatronics (AIM)*, Montreal, Canada, July 2010, pp. 303–310.

- [25] F. Aghili and C. Y. Su, “Robust relative navigation by integration of icp and adaptive kalman filter using laser scanner and imu,” *IEEE/ASME Transactions on Mechatronics*, vol. 21, no. 4, pp. 2015–2026, Aug 2016.
- [26] F. Aghili, “Automated rendezvous & docking (AR&D) without impact using a reliable 3d vision system,” in *AIAA Guidance, Navigation and Control Conference*, Toronto, Canada, August 2010.
- [27] H.-S. Choi, O.-D. Park, and H.-S. Kim, “Autonomous mobile robot using GPS,” in *Int. Conference on Control & Automation*, Budapest, Hungary, June 2005, pp. 858–862.
- [28] T. Kang-hua, W. Mei-ping, and H. Xiao-ping, “Multiple model kalman filtering for MEMS-IMU/GPS integrated navigation,” in *Industrial Electronics and Applications, 2007. ICIEA 2007. 2nd IEEE Conference on*, may 2007, pp. 2062–2066.
- [29] F. Aghili, M. Kuryllo, G. Okouneva, and C. English, “Fault-tolerant position/attitude estimation of free-floating space objects using a laser range sensor,” *IEEE Sensors Journal*, vol. 11, no. 1, pp. 176–185, Jan. 2011.
- [30] R. Lenain, B. Thuilot, C. Cariou, and P. Martinet, “Adaptive control for car like vehicles guidance relying on RTK GPS: Rejection of sliding effects in agricultural applications,” in *IEEE Int. Conf. On Robotics and Automation*, Taipei, Taiwan, September 2003.
- [31] F. Aghili, M. Kuryllo, G. Okouneva, and C. English, “Fault-tolerant pose estimation of space objects,” in *IEEE/ASME Int. Conf. on Advanced Intelligent Mechatronics (AIM)*, Montreal, Canada, July 2010, pp. 947–954.
- [32] F. Aghili, K. Parsa, and E. Martin, “Robotic docking of a free-falling space object with occluded visual condition,” in *9th Int. Symp. on Artificial Intelligence, Robotics & Automation in Space*, Los Angeles, CA, Feb. 26 – 29 2008.
- [33] F. Aghili, M. Kuryllo, G. Okuneva, and D. McTavish, “Robust pose estimation of moving objects using laser camera data for autonomous rendezvous & docking,” in *ISPRS Workshop Laserscanning*, Paris, France, September 2009, pp. 253–258.
- [34] F. Aghili and K. Parsa, “Adaptive motion estimation of a tumbling satellite using laser-vision data with unknown noise characteristics,” in *2007 IEEE/RSJ International Conference on Intelligent Robots and Systems*, Oct 2007, pp. 839–846.
- [35] F. Aghili and A. Salerno, *Multisensor Attitude Estimation and Applications*, 1st ed. CRC Press, 2016, ch. Adaptive Data Fusion of Multiple Sensors for Vehicle Pose Estimation.
- [36] F. Aghili, “3d simultaneous localization and mapping using IMU and its observability analysis,” *Journal of Robotica*, December 2010.
- [37] E. J. Lefferts, F. L. Markley, and M. D. Shuster, “Kalman filtering for spacecraft attitude estimation,” vol. 5, no. 5, pp. 417–429, Sep.–Oct. 1982.
- [38] M. E. Pittelkau, “Kalman filtering for spacecraft system alignment calibration,” vol. 24, no. 6, pp. 1187–1195, Nov. 2001.

- [39] S. P. Won and F. Golnaraghi, “A triaxial accelerometer calibration method using a mathematical model,” *Instrumentation and Measurement, IEEE Transactions on*, vol. 59, no. 8, pp. 2144–2153, 2010.
- [40] F. Aghili and K. Parsa, “Motion and parameter estimation of space objects using laser-vision data,” *AIAA Journal of Guidance, Control, and Dynamics*, vol. 32, no. 2, pp. 538–550, March 2009.
- [41] F. Aghili, M. Kuryllo, G. Okouneva, and C. English, “Robust vision-based pose estimation of moving objects for automated rendezvous & docking,” in *IEEE Int. Conf. on Mechatronics and Automation (ICMA)*, Xian, China, August 2010, pp. 305–311.
- [42] F. Aghili and K. Parsa, “An adaptive vision system for guidance of a robotic manipulator to capture a tumbling satellite with unknown dynamics,” in *IEEE/RSJ Int. Conf. on Intelligent Robots and Systems*, Nice, France, September 2008, pp. 3064–3071.
- [43] B. B. B. Southall and J. Marchant, “Controllability and observability: Tools for kalman filter design,” in *Proc. British Machine Vision Conference (BMVC '98)*, vol. 1, 1998, pp. 164–173.
- [44] F. Aghili, “Integrating IMU and landmark sensors for 3D SLAM and the observability analysis,” in *Proc. of IEEE/RSJ International Conference on Intelligent Robots and Systems (IROS)*, Taipei, Taiwan, Oct. 2010, pp. 2025–2032.
- [45] D. Goshen-Meskin and I. Y. Bar-Itzhack, “Observability analysis of piece-wise constant systems. i. theory,” *Aerospace and Electronic Systems, IEEE Transactions on*, vol. 28, no. 4, pp. 1056–1067, oct 1992.
- [46] M. Bryson and S. Sukkarieh, “Observability analysis and active control for airborne slam,” *Aerospace and Electronic Systems, IEEE Transactions on*, vol. 44, no. 1, pp. 261–280, january 2008.
- [47] F. Aghili, “3D SLAM using IMU and its observability analysis,” in *IEEE Int. Conf. on Mechatronics and Automation (ICMA)*, Xian, China, August 2010, pp. 377–383.
- [48] A. H. Jazwinski, *Stochastic Processes and Filtering Theory*. New York: Academic International Press, 1970.
- [49] P. S. Maybeck, *Stochastic Models, Estimation, and Control (Volume 2)*. New York: Academic Press, 1982.
- [50] C. K. Chui and G. Chen, *Kalman Filtering with Real-Time Applications*. Berlin: Springer, 1998, pp. 113–115.
- [51] R. G. Brown and P. Y. C. Hwang, *Introduction to Random Signals and Applied Kalman Filtering*. John Wiley & Sons, 1997, ch. The Discrete Kalman filter, State-Space Modeling, and Simulation, pp. 225–233.